

Automated robust registration of grossly misregistered whole-slide images with varying stains.

G. Litjens^{1,3}, K. Safferling^{1,2,3} and N. Grabe^{1,2,3}

¹Hamamatsu TIGA Center, Heidelberg, Germany;

²National Center for Tumor Diseases, Heidelberg, Germany;

³Steinbeis Transfer Center for Medical Systems Biology, Heidelberg, Germany;

ABSTRACT

Cancer diagnosis and pharmaceutical research increasingly depend on the accurate quantification of cancer biomarkers. Identification of biomarkers is usually performed through immunohistochemical staining of cancer sections on glass slides. However, combination of multiple biomarkers from a wide variety of immunohistochemically stained slides is a tedious process in traditional histopathology due to the switching of glass slides and re-identification of regions of interest by pathologists. Digital pathology now allows us to apply image registration algorithms to digitized whole-slides to align the differing immunohistochemical stains automatically. However, registration algorithms need to be robust to changes in color due to differing stains and severe changes in tissue content between slides. In this work we developed a robust registration methodology to allow for fast coarse alignment of multiple immunohistochemical stains to the base hematoxylin and eosin stained image. We applied HSD color model conversion to obtain a less stain color dependent representation of the whole-slide images. Subsequently, optical density thresholding and connected component analysis were used to identify the relevant regions for registration. Template matching using normalized mutual information was applied to provide initial translation and rotation parameters, after which a cost function-driven affine registration was performed. The algorithm was validated using 40 slides from 10 prostate cancer patients, with landmark registration error as a metric. Median landmark registration error was around 180 microns, which indicates performance is adequate for practical application. None of the registrations failed, indicating the robustness of the algorithm.

Keywords: histopathology, whole-slide imaging, image registration, prostate cancer

1. INTRODUCTION

Clinical histopathology has seen an increased use of immunohistochemical stains to aid in the diagnosis of cancer; a technique which can visualize individual proteins by using specific antibodies.^{1,2} For example, in breast cancer, using immunohistochemistry to assess the expression of estrogen receptor (ER) has become important in therapy selection for patients.³ One of the main disadvantages of using extra immunohistochemical slides in addition to the standard diagnostic hematoxylin and eosin (H&E)-stain is that it is cumbersome; pathologists had to switch out slides under the microscope and re-identify the relevant region they were looking at. The recent advent of digital pathology and whole-slide imaging has the potential to revolutionize the way pathologists use multiple stained slides. Because digital images of stained slides are acquired, pathologists can visualize multiple slides at once, either through multiplexing or side-by-side visualization using linked locations.

To allow multiplexing and linked slide positions, image registration is a prerequisite. Although a substantial amount of research has been done with regard to image registration in medical imaging, only a limited number of papers have focused on digital pathology. The most difficult challenges with regards to registration of immunohistochemical images, is that differing stains can result in a vastly different image appearance and that typically different sections are used, which means that they do not contain the exact same tissue content. Some researchers have already investigated image registration in immunohistochemical imaging. Mueller et al.⁴ applied real-time deformable registration with Elastix to differing immunohistochemical slides and showed good results with a median distance between expert annotated landmarks of 90 microns (global rigid transformation) and 20 microns (elastic registration). These results were later replicated by Lopez et al.⁵ Cooper et al.⁶ investigated a feature-based registration using adjacent slides to allow accurate feature matching. They showed that using their method overlap ratios between 0.89 and 0.95 could be achieved for manually annotated feature regions.

Although these studies show great results, they have some limitations for use in clinical practice. Often, especially in clinical trials, adjacent sections of the immunohistochemical stain and the H&E-stain are not readily available. Slides are often more than a couple of sections apart, which means that most local structures show significant change in appearance between slides. Furthermore, most slides are initially grossly misregistered, where tissue specimens are scanned upside down with respect to each other or even that multiple consecutive sections are present on the same slide. This means that for the accurate registration algorithms to be successfully applied, the initial coarse registration often has to be performed manually and direct application of the developed image registration algorithms will not give a satisfactory result.

In this study we developed an automated method which handles initial coarse registration of immunohistochemical images to the H&E-stained image and is robust to differing stains, tissue artifacts and large initial misalignment.

2. METHODOLOGY

The registration pipeline consists of four distinct steps: color conversion, background removal and selection of relevant tissue areas, initial alignment using template matching and final affine registration. This pipeline is applied to each immunohistochemically stained image to register it to the H&E-stained image. For the analysis up to the final affine registration a low-resolution version of the whole-slide images are used (downsample factor of 256 and 128 for images with an original resolution of 0.23 and 0.46 microns respectively). For the affine registration downsample factors of 64 and 32 were used.

2.1 RGB to HSD color conversion

The first step in the pipeline is to transform both the H&E-stained slide and the immunohistochemically stained slide from the RGB color space to the HSD color space.⁷ The main advantage of the HSD color space is that chromatic information and stain density are decoupled, significantly reducing the variation in image appearance between the slides.

For subsequent analysis, the chromaticity-independent density channel was used, which can be calculated straightforwardly using:

$$D_c = -\ln\left(\frac{I_c}{I_{0,c}}\right) \text{ and } D = \frac{D_r + D_g + D_b}{3} \quad (1)$$

where D_c is the density of color channel c , where c can be either R , G or B . D is the overall density.

Background removal and selection of relevant tissue areas The obtained density channel still contains preparation and scanning artifacts like air bubbles and some background intensity. To remove the background intensity a simple conservative thresholding procedure is applied on the density channel of the immunohistochemical and H&E images; all pixels with an optical density value below 0.2 are discarded. The resultant 'tissue mask' of the immunohistochemically stained image was subsequently processed using connected component analysis to get rid of in-slide templates and small artifacts like air bubbles by only retaining the largest connected component.

Sometimes several consecutive sections of tissue were present on the H&E-stained slide. We first registered one immunohistochemical image using our entire pipeline. This resulted in one tissue section on the H&E-slide which fitted best with this immunohistochemical section. For subsequent immunohistochemically stained sections we then automatically limited the registration to this H&E-section.

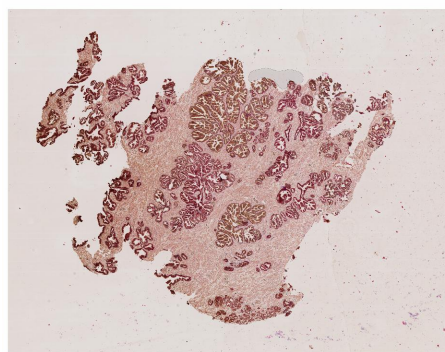
2.2 Initial alignment using template matching

Most image registration frameworks use cost function optimization to drive the registration process. However, if slides are initially have gross misalignment, simple strategies like initialization by matching the image centers do not work. We implemented a template matching routine to ensure good initial alignment. For the template matching routine, the density channel of the immunohistochemically stained image is moved along the density channel of the H&E-stained image at different rotation angles and translations.

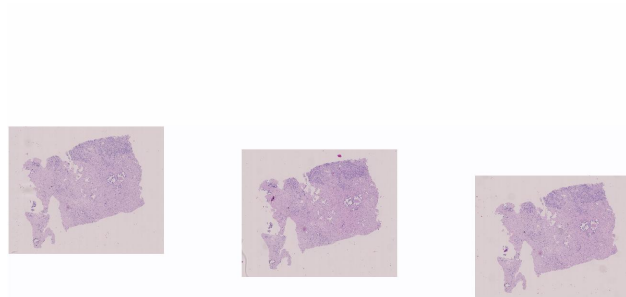
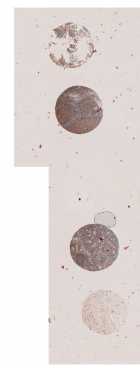
To evaluate how well the template 'fit' the H&E stained image we used normalized mutual information. Normalized mutual information allows us to further circumvent the issues with differing stains and has been



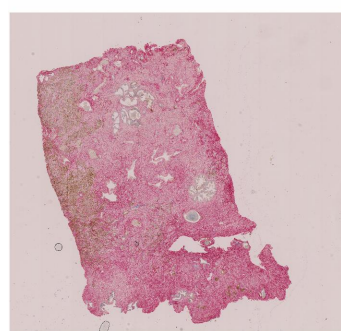
(a) H&E stained slide (patient 1)



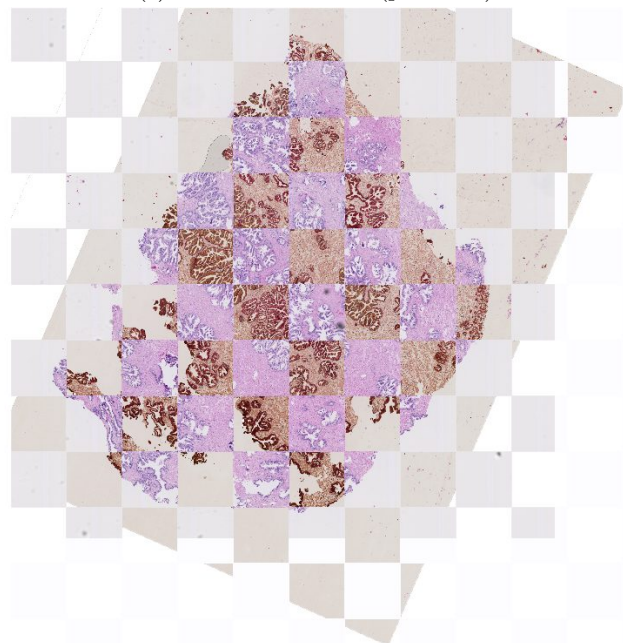
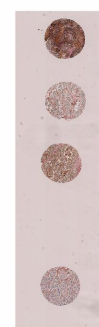
(b) iNOS-stained slide (patient 1)



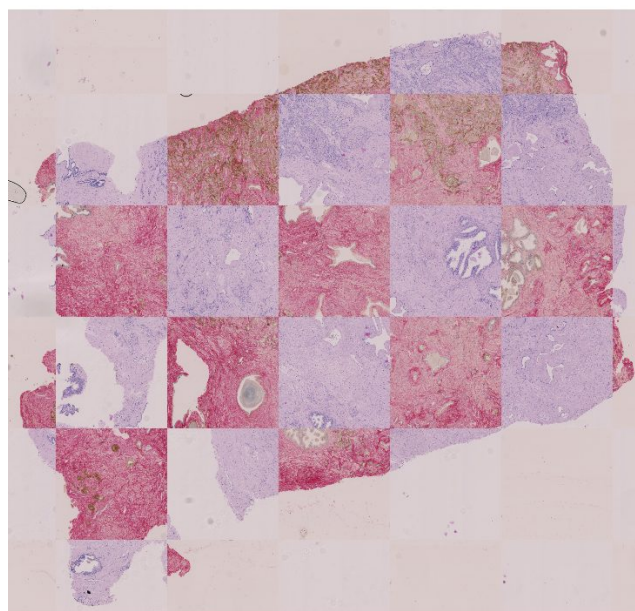
(c) H&E stained slide (patient 5)



(d) Col6A-stained slide (patient 5)



(e) Checkerboard (patient 1)



(f) Checkerboard (patient 5)

Figure 1: Example registration result for patient 1 and patient 5.

widely applied in image registration, for example in MRI.⁸ The template matching only uses two parameters: step sizes for the applied translation and rotation. We found step sizes of 20 pixels and $\frac{\pi}{4}$ to be the best compromise between detail and speed.

2.3 Affine registration

After initial alignment has been established by the template matching routine, a more thorough registration is applied to remove small rotation, translation and anisotropic scaling differences. Due to differing tissue preparation even consecutive sections often exhibit differences in tissue shrinkage and deformation. Although we do not attempt to remove these difference at the gland or cell level, we can remove it at the section level. To this end we used the elastix-framework,⁹ which has been previously applied to histopathology images.^{4,5}

For the affine transformation we used a multi-resolution pyramid with three levels with a downsample factor of two per level. The highest resolution level used in the affine registration was either the 64 or 32 times downsampled version of the full-resolution image (for the 0.23 and 0.46 micron resolution images respectively). Localized mutual information was used as the optimization metric with 32 histogram bins and stochastic gradient descent was chosen as the optimizer. A total of 2000 iterations were used per resolution level.

2.4 Validation

In total 40 slides were included from 10 prostate cancer patients. For each patient one H&E-stained slide with between 1 and 4 sections per slide was made. For each patient the H&E-stained slide and 3 out of 22 immunohistochemically-stained slides were selected (Col6A+CD276ab, Ki67+Keratin and iNOS+Keratin), such that they had varying locations within the specimen. All immunohistochemical slides were also counter-stained with hematoxylin. Slides were digitized using a Hamamatsu system at a resolution of 0.23 or 0.46 um per pixel.

For each slide an image analysis researcher with substantial experience in histopathology indicated between 5 - 7 corresponding points. Corresponding points were selected such that they indicated recognizable, larger structures, for example large prostate stones or large dilated glands. After subsequent registration of the immunohistochemical images to the H&E-stained image, the Euclidean distances in microns between the corresponding points was calculated. Furthermore, a visual assessment of registration accuracy was performed by checkerboard overlaying the registered images on the H&E-stained image.

3. RESULTS

Quantitative results on the landmark registration error are presented as box plots in Figure 2. Qualitative results for the slide with highest registration error and a slide with average registration error are show in Figure 1. The median landmark registration error across all patients is 181 microns whereas all registered points are within a 900 micron error, indicating that no registration failures occurred. These errors are already low enough to perform location matching between slides and allows coarse analysis of biomarker expression in larger regions of cancer, stroma or invasive margin. Higher accuracy can be achieved by performing a successive higher resolution local affine or elastic registration technique.

4. DISCUSSION

In this paper we presented a fully automated method to register non-adjacent, grossly misregistered whole-slide histopathology images. Our results indicate that a reasonable average registration error of 181 microns could be obtained without any registration failures.

The accuracy of our method is mostly limited by a relatively small amount of large landmark registration errors usually (up to 850 microns) typically occurred due to partly missing or destroyed tissue. Figure 1ab shows a good example, where the bottom part of the immunohistochemical slide is for a large part torn/destroyed. Only local elastic registration of these regions might able to reduce landmark errors in these cases.

One main limitation is that only one observer annotated landmarks in this study, and thus observer error is also contained within the landmark registration error. Observer error can be substantial in difficult cases and as such an accurate assessment of intra- and inter-observer variability should be performed in future studies.

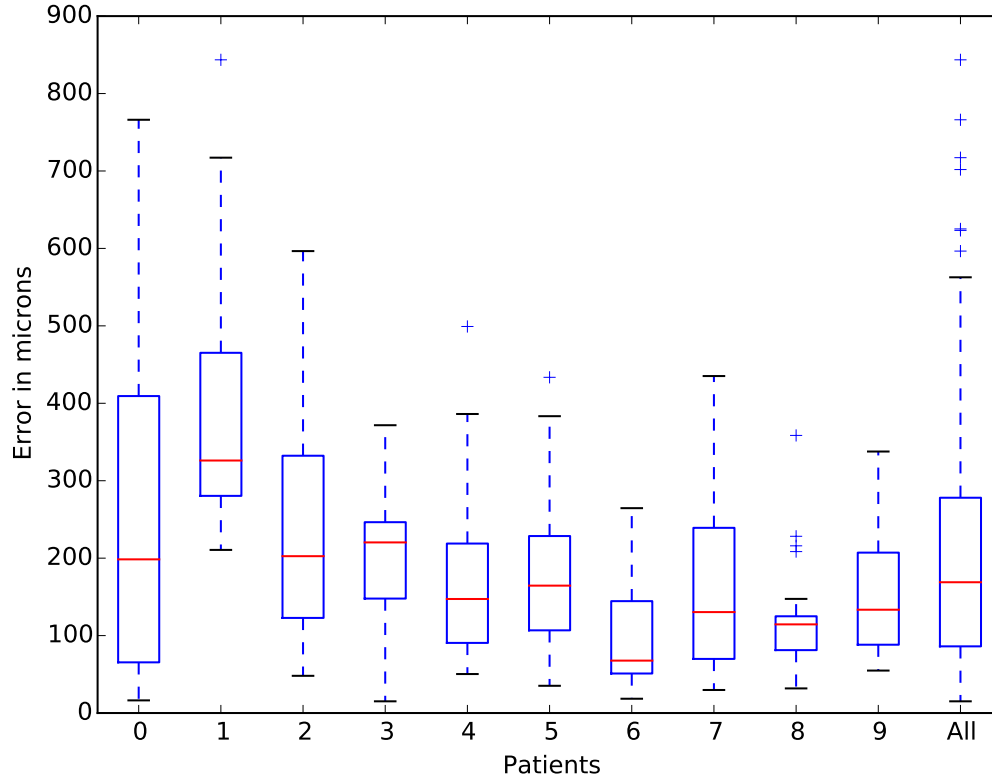


Figure 2: Boxplot of the landmark registration error in microns over ten patients with three immunohistochemically stained slides each. Each slide had between 5 - 7 landmarks for a total of 165 landmarks.

As all studies currently published on co-registering immunohistochemistry and H&E-stained images focused on adjacent slides, a fair comparison is difficult. Furthermore, only one other study reported landmark registration error. They found an average registration error of around 90 microns, which is approximately half of the error obtained in this study. However, as they used adjacent sections, relatively nicely pre-aligned slides, and other data a real comparison is not possible. Summarizing, we have presented a fast registration method for initial coarse alignment of immunohistochemical slides to H&E-stained slides which is robust to differing stains and large changes in tissue architecture.

REFERENCES

- [1] Leonard, G. D. and Swain, S. M., "Ductal carcinoma in situ, complexities and challenges," *J Natl Cancer Inst* **96**, 906-920 (2004).
- [2] Halama, N., Zoernig, I., Spille, A., Westphal, K., Schirmacher, P., Jaeger, D., and Grabe, N., "Estimation of immune cell densities in immune cell conglomerates: an approach for high-throughput quantification," *PLoS One* **4**, e7847 (2009).
- [3] Fujimura, T., Takahashi, S., Urano, T., Kumagai, J., Ogushi, T., Horie-Inoue, K., Ouchi, Y., Kitamura, T., Muramatsu, M., and Inoue, S., "Increased expression of estrogen-related receptor alpha (erralpha) is a negative prognostic predictor in human prostate cancer," *Int J Cancer* **120**, 2325-2330 (2007).
- [4] Mueller, D., Vossen, D., and Hulsken, B., "Real-time deformable registration of multi-modal whole slides for digital pathology," *Comput Med Imaging Graph* **35**, 542-556 (2011).

- [5] Moles Lopez, X., Barbot, P., Van Eycke, Y.-R., Verset, L., Trépant, A.-L., Larbanoix, L., Salmon, I., and Decaestecker, C., "Registration of whole immunohistochemical slide images: an efficient way to characterize biomarker colocalization," *J Am Med Inform Assoc* **22**, 86–99 (2015).
- [6] Cooper, L., Sertel, O., Kong, J., Lozanski, G., Huang, K., and Gurcan, M., "Feature-based registration of histopathology images with different stains: an application for computerized follicular lymphoma prognosis," *Comput Methods Programs Biomed* **96**, 182–192 (2009).
- [7] van der Laak, J. A., Pahlplatz, M. M., Hanselaar, A. G., and de Wilde, P. C., "Hue-saturation-density (HSD) model for stain recognition in digital images from transmitted light microscopy," *Cytometry* **39**, 275–284 (2000).
- [8] Viola, P. and Wells III, W. M., "Alignment by maximization of mutual information," *Int J Comput Vis* **24**, 137–154 (1997).
- [9] Klein, S., Staring, M., Murphy, K., Viergever, M. A., and Pluim, J. P. W., "elastix: a toolbox for intensity-based medical image registration," *IEEE Trans Med Imaging* **29**, 196–205 (2010).